# RADIOLOGICAL PROTECTION CALCULATIONS OF THE ELI-NP 10 PW LASER EXPERIMENTAL AREA USING FLUKA CODE

M. A. POPOVICI[1], F. NEGOITA[2, 3], I. O. MITU[3, *], R. VASILACHE[4, *], D. BUZATU[1]

[1]Physics Department, *Politehnica* University of Bucharest, Splaiul Independenţei 313, RO-060042, Bucharest, Romania
Emails: maria-ana.popovici@physics.pub.ro, daniela.buzatu@physics.pub.ro
[2]*Horia Hulubei* – National Institute for Physics and Nuclear Engineering, Reactorului 30, P.O.BOX MG-6, Bucharest – Măgurele, Romania
Emails: florin.negoita@eli-np.ro
[3]Extreme Light Infrastructure – Nuclear Physics, Reactorului 30, P.O. Box MG-6, RO-077125, Bucharest-Măgurele, Romania
Emails: iani.mitu@eli-np.ro, florin.negoita@eli-np.ro
[4]*Canberra Packard Ltd.* – 18 Clejani St., 051036 Bucharest, Romania
Emails: r.vasilache@cpce.net
**Corresponding authors: iani.mitu@eli-np.ro, r.vasilache@cpce.net*

*Abstract*. The high levels of ionizing radiation expected at most of the experimental areas of the Extreme Light Infrastructure - Nuclear Physics (ELI-NP) facility in Bucharest are challenging from a radiation protection point of view. FLUKA Monte Carlo code is a widely used tool allowing to estimate dose contributions of the complex radiation fields and the transport of the radiation through the bulk shielding. In this paper we present the results of a shielding study for the experimental area E1, the site of the laser driven nuclear physics experiments. Updated source terms were used and ambient dose equivalent rates were calculated to check the compliance with the design target dose values and to identify critical dose locations. To reduce radiation levels for neighbouring areas below the required limits, an optimized beam dump and local shielding were proposed.

*Key words* - radiation protection, Monte Carlo simulation, FLUKA, shielding, ELI-NP

## 1. INTRODUCTION

ELI-NP (Extreme Light Infrastructure - Nuclear Physics) is designed to become the most advanced research facility in the ultra-high intensity laser physics field. The main goal of this infrastructure is the study of nuclear physics and its applications, using high power laser systems and a high energy gamma beam. This unique combination of experimental setups will enable ELI-NP to tackle a wide range of research topics in fundamental physics, nuclear physics and astrophysics, and also applied research in materials science, management of nuclear materials and life sciences [1]. ELI-NP facility consist of two components: a) a very high intensity laser system, with two 10 PW laser arms able to reach intensities of $10^{23}$ W/cm$^2$, and electrical fields of $10^{15}$ V/m; b) a very intense ($10^{13}$ γ/s), brilliant γ beam, ~ 0.1 % bandwidth, with γ-ray energy up to 19.5 MeV [2], [3]. Due to the ultra-high laser power and intensities, high energy γ-rays, charged particles and neutrons could be produced, inducing further various nuclear reaction products relevant for radioprotection. At ELI-NP the studies in the E1 experimental area will benefit from High Power Laser System pulses and will focus on Laser Driven Nuclear Physics [4].

Our simulations are related to the radiological studies in E1 area. Thus, we computed all particle dose equivalent rate values in μSv/h to determine the location of the hot zones, the primary and secondary fluence maps, to allow for a correct choice of the detectors types that are going to be used for radiation monitoring. Some of the source terms described in the Technical Design Reports [4], [5] were used for our simulations. A realistic modeling of the above mentioned experimental area, by using data from the latest version of the AutoCAD drawing files of the ELI-NP building has been implemented in FLUKA Monte Carlo radiation transport code [6], [7]. Good knowledge of the complex radiation field is decisive for placing the control and measuring equipment in the entire experimental building. Similar shielding studies were previously done both for the Romanian [8] and Czech [9], [10] pillars of the ELI European Project.

## 2. E1 EXPERIMENTAL AREA

E1 belongs to the joint E1/E6 area of the ELI-NP building where experiments using the two arms of the 10 PW high intensity laser system will be performed. It is dedicated mainly to laser induced nuclear reactions in solid targets. From a radiological point of view E1 is highly challenging, because the expected radiation fields exhibit unique properties of composition, energy and spatial distributions. Thus, beams of energetic charged and neutral particles with a wide spatial disposition will be obtained simultaneously. Calculations performed at the E6 area showed that if one considers sources of equal intensity and energy range, but different with respect to the spatial disposition (a narrow and a wide spread beam were considered separately), the latter will produce higher dose equivalent rate values at positions of interest inside and outside the bulk shielding [8]. It is reasonable to assume that a similar, or even less favourable shielding case will occur at E1.

E1 experimental area - Figure 1(a) and (b) is located in a bunker with 2-m-thick lateral walls and 1.5-m-thick floor and ceiling. Access to the bunker is provided by 2-m-thick shielding doors. The laser - target interaction will occur in a parallelepiped shaped interaction chamber (IC), having 10 cm thick walls, made of a special aluminium alloy - Al6061, with good mechanical, thermal, and low activation properties. Primary beams generated inside the IC will be extracted through vacuum removable windows (60-cm-diameter and 2-mm-thick in the current modelling), and will be stopped in a beam dump (BD) which is also designed to absorb secondary radiation produced in nuclear physics experiments taking place at E1 experimental area. BD has a parallelepiped display, with large transverse dimensions (560 cm x 350 cm), in order to "cover" expected radiation sources with broad spatial distributions. Its composition is graphite (80 cm)/aluminium (300 cm) layers in an iron casing (10 cm).

The primary beam particles considered in this study were: 1) protons (flat energy distribution in the range 0 - 500 MeV, and a number of particles per laser pulse of $1.4\times10^{12}$ protons/pulse), and 2) electrons (Gaussian energy distribution at an average value of 1.5 GeV, FWHM 10%, and a number of particles per pulse of $8\times10^{10}$ electrons/pulse). The flux values expressed in number of particles per second, which were used to normalize the "per primary" FLUKA results in order to obtain dose equivalent and fluence rate values, were calculated by considering a laser frequency of 1 pulse/min. The proton source term represents an update of the 0 - 100 MeV flat energy

distribution which was used in the preliminary calculations for the bulk shielding design. The electron source term describes the accompanying negatively charged particles which result from the laser pulse - target interaction [5]. For both sources the radiation was emitted in a cone of $20^{\circ}$ divergence half-angle.

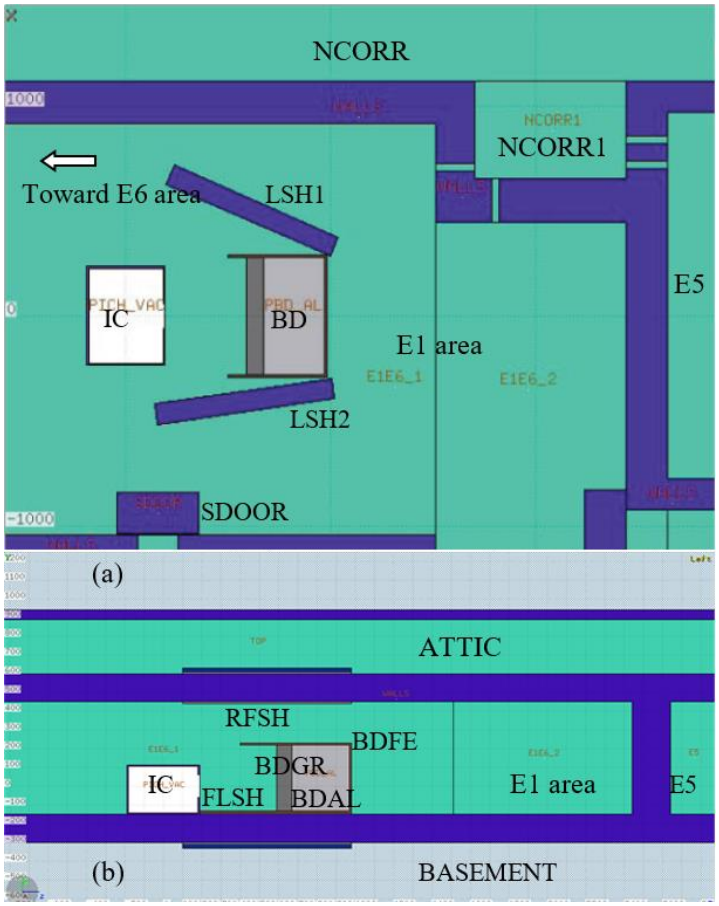


Fig. 1 – E1 experimental area layout - geometry in Flair. (a) Horizontal representation at the beamline level (b) Vertical representation through the beam source position. Notations: NCORR, NCORR1 - regions in the north corridor, E5 - adjacent experimental area, IC - interaction chamber, SDOOR - shielding door to south area, BD – beam dump, LSH1, LSH2 - local shielding; RFSH - roof local shielding, FLSH - floor local shielding, BDGR – beam dump graphite; BDAL – beam dump aluminium , BDFE – beam dump iron. The figure was obtained by using Flair, the graphical interface for FLUKA [11].

Calculations using a simplified geometry, where only the walls, the interaction chamber, and the beam dump were present, showed that for each of the source terms we considered, "hot zones" were produced, where the equivalent dose rate values due to all particles in the complex radiation field were well beyond the design constraint values. These values are 2 mSv/year (occupational) and 0.1 mSv/year (public), which represents 1/10 of

the values given in the BSSD [12] and the Romanian legislation. In order to fix the problem of the dose constraint exceedance in area with expected high level occupancy such as corridors, local shielding elements were added. Thus, two lateral ordinary concrete barriers (1 m thick) LSH1, LSH2 were placed in the vicinity of the beam dump - see Figure 1(a), to protect experimental areas and corridors surrounding E1. The most significant amount by which the calculated dose exceeds the required limit was found between IC and BD, immediately above the floor. Also, a corresponding "hot zone" exists at the ceiling level, with a less elevated dose, due to longer distance from the radiation source. In order to cut down dose values in the basement and in the attic, local shielding against photons and neutrons (10 cm lead and 20 cm borated polyethylene layers) was added at the floor (FLSH) and roof (RFSH) levels.

## 3. FLUKA SHIELDING STUDY RESULTS

Figure 2 (a) and 2(b) shows maps of ambient dose equivalent rate values $\mathrm{d}H^*(10)/\mathrm{d}t$ in $\mu\mathrm{Sv}/\mathrm{h}$ generated by the most problematic radiation source - the protons.

(a)

(b)

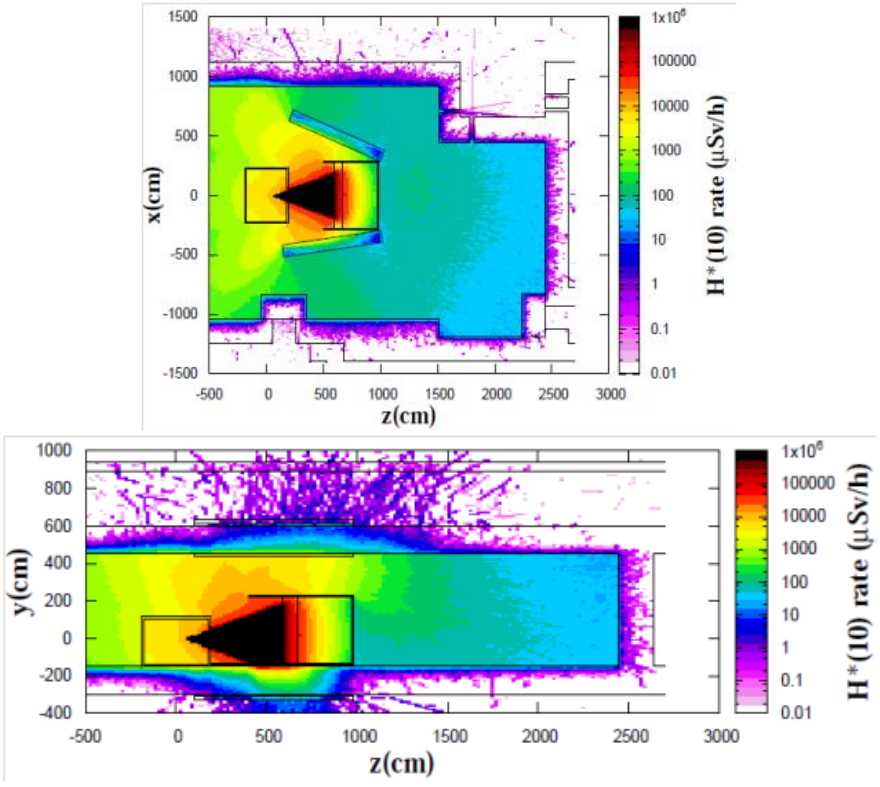


Fig. 2 – Map representation of the total dose equivalent rate d$H$*(10)/d$t$ in μSv/h given by the proton source term in the (a) horizontal and (b) vertical sections throughout E1 and neighboring areas, at the beam height level and through the beam position, respectively.

The results were obtained by using a parallelepiped shaped sampling volume which spans a horizontal section of E1, located at the beam level - 2(a), and a vertical one, at the beam source position - 2(b). The individual bin sizes were 15cm x 15 cm x 15cm. FLUKA "pSv per primary" results were converted to μSv/h by considering the assumed $1.4\times10^{12}$ protons/pulse at a laser pulse frequency of 1 pulse/minute. The representative sections were chosen after examining the volume data, which revealed that maximum total dose values are achieved in these planes. From Figure 2 (a) it can be observed that the BD and the lateral concrete structures LSH1, LSH2 provide the required shielding of E1 neighboring areas: north corridor, E5, access areas - see Figure 1 (a) and 1(b).
However, typical ambient dose equivalent rate values of the prompt radiation field inside E1, behind the designed stoppers are very elevated, of approximately hundreds of $\mu Sv/h$ , and the presence of the 2-m thick bunker walls is mandatory in order to contain the radiation field inside the experimental area. In Figure 2(b) the dose rate map presents an even less favorable situation. The dose maxima on the hot side of the lower and upper areas of the bunker are exceedingly high: $10^6$ μSv/h at the floor level and $10^4$ μSv/h at the roof. The designed local screens and the 1.5-m thick floor and roof slabs reduce the dose rate values by 5 and 4 orders of magnitude, respectively.

To obtain more precise information and check the compliance with the dose constrain, we used one-dimensional total dose equivalent rate graphs, as presented in Figure 3(a) and 3(b).

According to Figure 3(a), on the hot side of the roof slab, the dose (continuous line/point curve) does not decrease below the limit value. The dose maxima (up to $10^4$ $\mu Sv/h$ ) are obtained between the IC and the BD. The secondary radiation is completely absorbed laterally, in the 2-m-thick wall separating E1 from E5. The same graph shows that on the cold side of the roof slab (dotted line/point curve) there is a "hot region" where the dose rate values are a few $\mu Sv/h$ . Its dimension in the beam direction is of approximately 10 m, starting 1 m away from a position corresponding to the window of the IC.

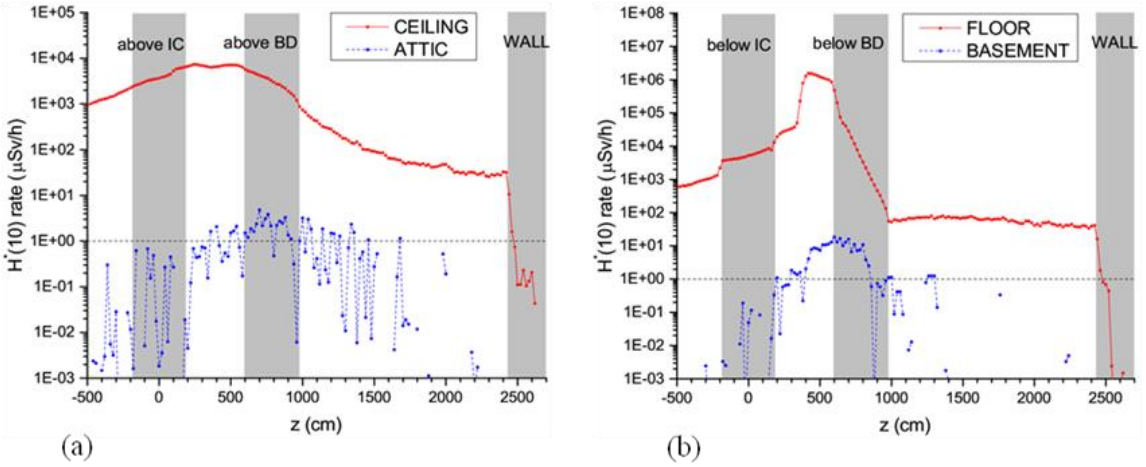


Fig. 3 – Total *H**(10) rate in μSv/h generated by the proton source term in the volume of a 15 cm x 15 cm (xy section) column which spans the length of the geometry (z direction) and is located: (a) above the beamline, at the ceiling level (the hot side) and above the roof slab, in the attic (the cold side), correspondingly; (b) below the beamline, at the floor level and below the floor slab, in the basement. For spatial orientation, the limits of the occupied areas were marked by vertical lines and regions were labelled.

The dose rate values corresponding to the floor sampling column are presented in Figure 3(b). The maximum dose values obtained here go beyond $10^6$ μSv/h , which is about two orders of magnitude more than the dose obtained in corresponding zones at the ceiling level. This is understandable if we consider the much shorter distance from the radiation source position. It can be observed that the BD reduces the dose rate values by approximately 4 orders of magnitude, but they never get below $10^2$ μSv/h on the hot side of the floor slab. The same combined lead and borated polyethylene local protection was used to bring the total dose on the cold side of the floor within the admitted range, as seen in Figure 3(b), apart from a hot zone which can be found in the space between the IC and the BD.

In conclusion, in the attic and in the basement localized hot spots are still present beyond the bulk and local shielding. Whilst in the attic, the hot spots do not significantly exceed 1 μSv/h (values which are up to 3 - 4 μSv/h , thus still within the limits of instantaneous dose rates usually imposed by the regulatory body), the hot spots in the basement are significantly higher and can reach tens of μSv/h . This is why both the attic and especially the basement have to be declared controlled areas and have the access limited to the "off-time" periods.

The 1D representation of the results concerning the less difficult source term of electrons are presented in Figure 4 (a) and (b).

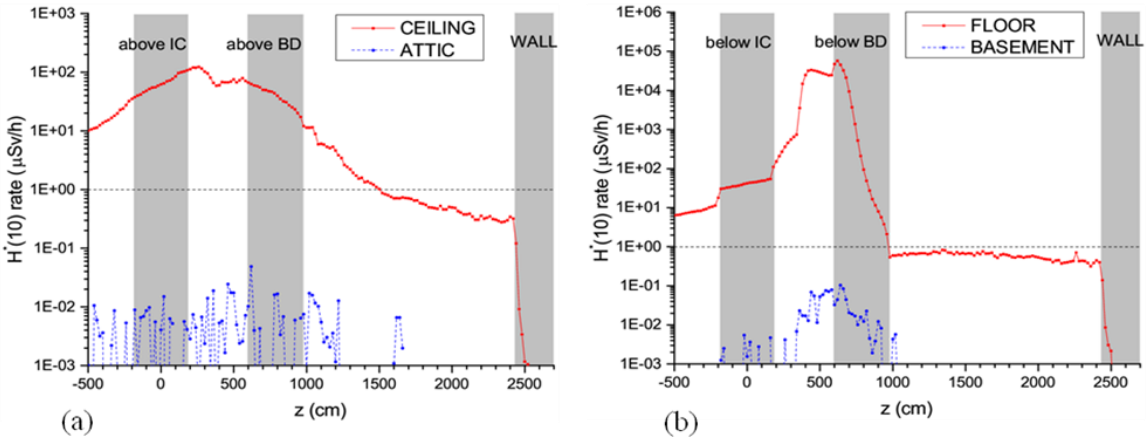


Fig. 4 – Similar to Figure 3, for the electron source term

According to Figure 4(a), on the hot side of the roof slab, the dose (continuous line/point curve) decreases below the limit value over approximately 5 m measured behind the rear side of the BD, which is located at a distance of 15m from the wall which separates E1 and E5. The dose rate at the inner wall surface is so low that the radiation is completely absorbed in 50cm of the 2-m-thick barrier. However in the zone above the BD and the IC, dose values are obtained that exceed the constraint [4] of $1\,\mu\mathrm{Sv/h}$ by two orders of magnitude. The proposed BD and RFSH make the dose on the cold side of the roof slab (dotted line/point curve) 3-4 orders of magnitude less than the limit.

In Figure 4(b) it can be noticed that the BD absorbs completely the incident radiation, so that the dose on the hot side of the floor falls below $1\,\mu\mathrm{Sv/h}$ right behind the BD. The most problematic areas correspond again to the space delimited by the window of the IC and the BD, where dose values are 2 orders of magnitude higher than at the corresponding location, on the hot side of the roof - Figure 4(a). The same combined lead and borated polyethylene local protection was used to bring the dose on the cold side of the floor within the admitted range, as seen in the figure.

Altogether, Figures 4(a) and 4(b) show that the local shielding elements reduce the dose rates to normal values (within tens of nSv/h) in all those areas where personnel might have access, thus keeping the exposure within background level limits.

A description of the main prompt radiation field components generated by the considered proton source at E1 is given in Figure 5, by map representation of the fluence rate values $\left(\#/\mathrm{cm}^2/\mathrm{s}\right)$ throughout this experimental area. For this particular source of radiation, most secondaries were generated in nuclear reactions. According to FLUKA output files, most of the nuclear reactions were generated by protons (around 54%) and by neutrons (around 45%). In the inelastic interactions of primary protons an important fraction of the total number of secondary per beam particles is represented by $\alpha-$particles (around 24.5%),

protons (around 26.6%), photons (around 13.6%) and neutrons (around 26.4%). The primary proton energy loss is due mainly to Coulomb interaction processes $\mathrm{d}E/\mathrm{d}x$ (around 84%). Apart from those, there is a small fraction of electromagnetic showers - only around 7% of the average energy (250 MeV) is spent in these processes. Nuclear recoils, heavy fragments (around 0.9%) and low energy neutron reactions (around 0.6%) are also produced.

In Figure 5, the neutron and photon fluence rate values were represented both in a horizontal and vertical projection containing the beam position. As expected, on the cold side of the bulk shielding, only neutrons and photons can be found. They produce the hot spots previously described in terms high dose equivalent rate values. Inside the E1 experimental area, neutron fluence exhibits larger values than photon fluence. This is opposite to the case of secondaries produced by the electron source term (not presented here), where photon fluence is more important than the neutron fluence, mainly due to a more significant electromagnetic shower presence. In Figure 5 it can also be observed that the charged particles - electrons, positrons, and protons are readily contained inside the bunker by the designed shielding.

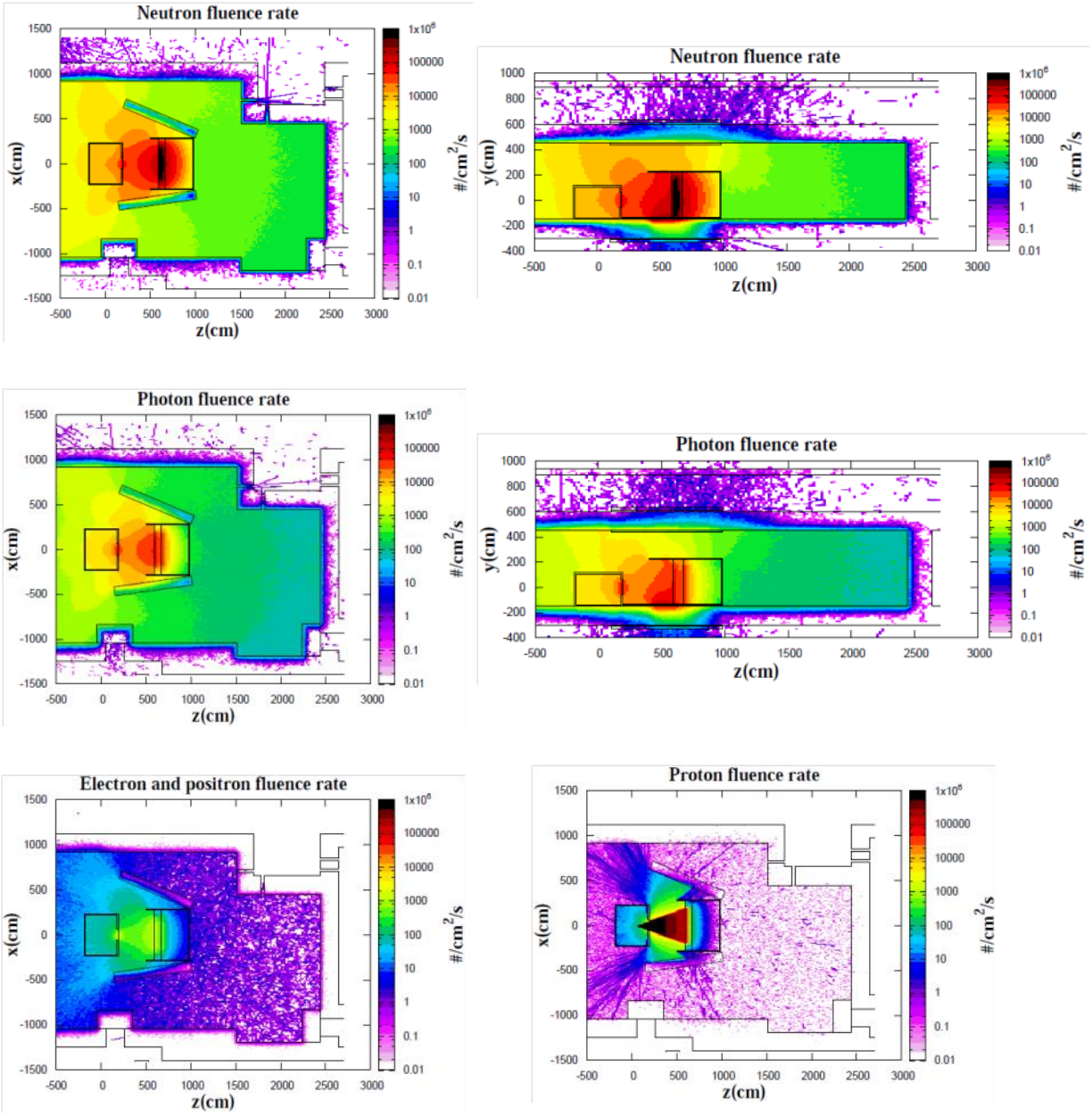


Fig. 5 – Secondary prompt radiation field components produced by the proton source term: neutrons, photons, electrons and positrons, protons. Particle fluence rate expressed in #/cm$^2$/s. To normalize FLUKA "per primary" results, a flux value of 2.33 x $10^{10}$ protons/s was considered. The proton scoring includes the primaries as well. For the most important components: neutrons and photons, fluence rate values are represented both in a horizontal section, at the beamline height (left), and in a vertical section through the beam source position (right).

## 4. CONCLUSIONS

In this study we used FLUKA Monte Carlo transport code calculations to determine the critical dose locations, and the primary and secondary particle fluence maps which are necessary for a correct choice of the detector types to be used in the E1 experimental area of the ELI-NP building.

Map representations were obtained for the total ambient dose equivalent rate values $\mathrm{d}H^*(10)/\mathrm{d}t$ in $(\mu\mathrm{Sv/h})$ given by the proton and electron source terms, in horizontal and vertical cross sections throughout E1. The number of beam particles per laser pulse used in the data processing were: $1.4\times10^{12}$ protons/pulse for the proton beam with a 0 - 500 MeV flat energy distribution, and $8\times10^{10}$ electrons/pulse for the electron beam with a Gaussian distribution of 1.5 GeV average value and 10% FWHM, at a 1 pulse/min repetition rate of the laser pulses.

For the primary proton beam, the ambient dose equivalent rate values obtained inside the bunker can reach high levels, of order $100\,\mu\mathrm{Sv/h}$, even behind the BD. The 1D graph representations given in Figures 3(a) and 3(b) indicate the presence of problematic areas on the hot side of the ceiling and floor slabs, between the IC and the BD. The dose values obtained in those regions exceed the imposed constraint for accessible area during experiment by 6 and 4 orders of magnitude, respectively, imposing restriction of access in those areas. In spite of the presence of local shielding, on the cold side of the bunker, in the attic and the basement hot spots were obtained, where dose values reach 3 - 4 μSv/h and tens of μSv/h, respectively. According to Figure 5, they are produced by the secondary neutron and photon radiation fields. Further protective measures, like declaring those regions controlled areas, where access is limited to the "off-time" periods, are to be taken.

It can be noticed that for the primary electron beam, the total radiation field is readily contained inside the experimental area; the beam dump and the lateral concrete structures LSH1, LSH2 provide an effective shielding of E1 neighbouring areas: north corridor, E5, access areas, etc. Typical ambient dose equivalent values of the prompt radiation field behind the designed stoppers are of approximately $0.5\,\mu\mathrm{Sv/h}$.

A description of the secondary prompt radiation field components (electrons-positrons, neutrons, protons and photons) generated by the proton source at E1 is given by map representation (Figure 5) of the fluence rate values $(\#/\mathrm{cm}^2/\mathrm{s})$ throughout this experimental area.

This work was supported by a grant in the programme: 5/5.1/ELI-RO, project type: ELI-04/19.10.2017. I. O. Mitu and F. Negoita were supported by the Project Extreme Light Infrastructure – Nuclear Physics (ELI-NP), a project co-financed by the Romanian Government and European Union through the European Regional Development Fund.

REFERENCES

1. N.V. Zamfir, Nuclear Physics with 10PW laser beams at Extreme Light Infrastructure – Nuclear Physics (ELI–NP), Eur. Phys. J. Special Topics, vol 223, 2014, pp. 1221-1227

2. D. L. Balabanski, G. Cata-Danil, D. Filipescu, S. Gales, F. Negoita , O. Tesileanu, C. A. Ur, I. Ursu, N. V. Zamfir, Towards experiments at the new ELI-NP facility, EPJ Web of Conferences, vol. 78, 2014, pp. 06001-06007
3. ELI-NP White Book. http://www.eli-np.ro/documents/ELI-NP-WhiteBook.pdf
4. F. Negoita & all, Laser Driven Nuclear Physics at ELI–NP, Romanian Reports in Physics, Vol. 68, Supplement, P. S37–S144, 2016
5. I. O. Mitu et al., Radiation Protection and Safety at ELI–NP, Rom. Rep. in Phys., vol. 68, Supplement, 2016, pp. S885-S945
6. A. Ferrari, P.R. Sala, A. Fasso`, J. Ranft, FLUKA: a multi-particle transport code" CERN-2005-10, 2005, INFN/TC_05/11, SLAC-R-773
7. T.T. Böhlen, F. Cerutti, M.P.W. Chin, A. Fassò, A. Ferrari, P.G. Ortega, A. Mairani, P.R. Sala, G. Smirnov, V. Vlachoudis, The FLUKA Code: Developments and Challenges for High Energy and Medical Applications, Nuclear Data Sheets vol. 120, 2014, pp. 211-214
8. M. A. Popovici et al., Shielding assessment of high field (QED) experiments at the ELI-NP 10 PW laser system, J. Radiol. Prot., vol. 37, 2017, pp 176–188
9. A. Ferrari, E. Amato, D. Margarone, T. Cowan, G. Korn Radiation field characterization and shielding studies for the ELI Beamlines facility, Applied Surface Science,vol 272, 2013, pp. 138-144
10. V. Olšovcová, R. Haley, L. MacFarlene, B. Rus, M. Griffiths, Bulk shielding for laser research centre ELI Beamlines, Applied Surface Science,vol 4, 2014, pp. 247-251
11. V.Vlachoudis, FLAIR: A Powerful But User Friendly Graphical Interface For FLUKA, Proc. Int. Conf. on Mathematics, Computational Methods & Reactor Physics (M&C 2009), Saratoga Springs, New York, 2009
12. International Basic Safety Standards for Protection against Ionizing Radiation and for the Safety of Radiation Sources, Safety Series No. 115, IAEA, Vienna (1996). http://www.ilo.org/wcmsp5/groups/public/@ed_protect/@protrav/@safework/documents/publication/wcms_152685.pdf